



# Safety Analysis and Water Control Strategies for Roadway Excavation in Coal Mining Faces under Extremely Thin Bedrock

Zhida Liu<sup>1</sup>

<sup>1</sup>Zaozhuang Vocational College of Science and Technology, Tengzhou, Shandong  
liuzhidachina@163.com

**Abstract.** The average thickness of the main mined 3<sup>#</sup> coal seam in a Shandong mine is 8.5m. According to the mine's future production succession plan, the 7-1 working face will be mined next. The minimum bedrock thickness in this area is only 22 m, increasing the threat of water and sand inrush from the Quaternary loose layer. To avoid induced water and sand inrush disasters during shallow roadway excavation and construction, and to ensure construction safety, this study analyzes the mining conditions, geological conditions, and hydrogeological conditions of the fault-affected thin-bedrock coal roadway. By integrating analytical methods and numerical calculations, the overlying strata failure height after roadway excavation is comprehensively determined. A water prevention and control safety evaluation of roadway excavation is conducted, achieving safe excavation.

**Keywords:** Fault, Roadway Excavation, Water Prevention and Control, Thin Bedrock

## 1 Engineering Background

The 7-1 working face is a first-sublevel working face of the No. 3 coal seam. The thickness of the roof bedrock ranges from 22 m to 53 m. Both the track roadway and transportation roadway of the 7-1 working face are designed for excavation along the roof of the No. 3 coal seam, with rectangular cross-sections of 3.6 m×2.5 m (length×height) (see Fig. 1).

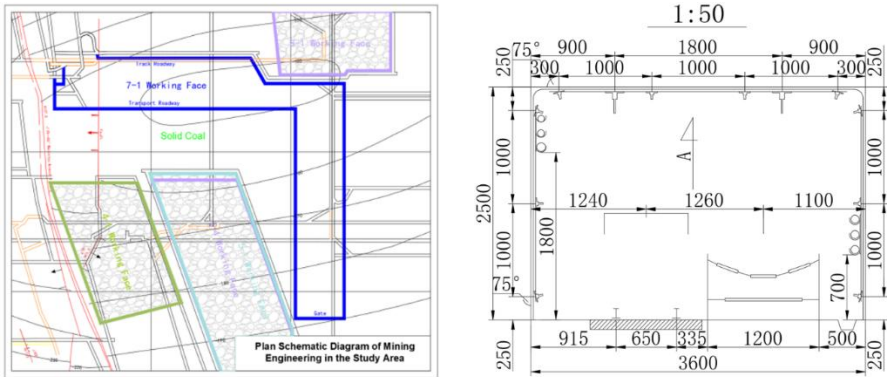


Fig. 1. Overview of the Study Area

## 2 Analysis of Hydrogeological Conditions

### 2.1 Occurrence Characteristics of Loose Strata in the Working Face

Based on original surface and underground borehole data near the 7-1 working face, combined with interpolation algorithms, the overlying Quaternary strata were calculated to be 156.2–180.0 m. The strata exhibit relatively uniform distribution in the middle but significant spatial variability at both ends. Along the working face advance direction, the thickness first slightly increases, then decreases, and subsequently gradually increases again, with the minimum thickness anticipated is at the northern corner. The bottom clay layer within the Quaternary strata is 0.6–3.2 m, with its thickness following a similar trend: first increasing, then decreasing, and then increasing again, with the minimum thickness occurring at the working face corners. The favorable clayey composition endows the strata with the capacity to withstand mining-induced impacts, obstructing the migration of water and sand from overlying aquifers.

### 2.2 Analysis of Water-Bearing Capacity of Overlying Strata in the Working Face

- (1) The Quaternary strata near the 7-1 working face are divided into upper and lower groups. The lower group aquifer exhibits weak water-bearing capacity. Notably, the specific water yield (unit discharge) during pumping tests in the lower Quaternary aquifer at Borehole Ke-5 is 0.0029 L/s·m, indicating extremely weak water-bearing capacity.
- (2) Among 25 underground Quaternary exploration wells near the 7-1 working face, 3 yielded no water when reaching the bottom aquifer of the Quaternary strata. Of the 23 nearby wells, 19 exhibited no water or only dripping/seepage, while 4 displayed minimal inflow (0.1–0.5 m<sup>3</sup>/h) that rapidly diminished to seepage. Thus, the bottom aquifer of the Quaternary strata overlying the 7-1 working face exhibits weak water-bearing capacity.

(3) Analysis of historical hydrogeological data from Baodian Coal Mine (Table 1, Fig. 2) reveals that from December 2008 to March 2024, the water level in the bottom aquifer of the Quaternary strata at Borehole Lower Q-17 declined from -83.82 m to -94.3m (a total decline of 10.48 m). The annual decline in water level indicates gradual attenuation of water-bearing capacity and poor hydraulic connectivity within the overlying loose strata.

### 2.3 Analysis of Occurrence Characteristics and Water-Bearing Capacity of Bedrock Pillar

(1) Statistical analysis of borehole data shows 7-1 working face bedrock thickness ranges 22–53 m, thinnest at northern track roadway. Mudstone constitutes 38.2% of bedrock, mainly in middle-upper sections, forming a "soft upper-hard lower" structure with the weathered top zone.

(2) The No. 3 coal seam immediate roof (mudstone-siltstone interbedding) has compressive strength 39.5 MPa, tensile strength 1.34 MPa, and collapses during initial caving. The main roof (medium sandstone) features 47.4 MPa compressive strength, 3.86 MPa tensile strength, and expands the caving zone upward with increased mining thickness. Fracture mechanics shows "hard-soft-hard" strata optimally suppress crack propagation: hard layers resist initiation, soft layers dissipate energy, and overlying hard layers terminate growth. The study area's alternating structure enhances sand-proof pillar safety.

(3) Borehole pumping tests indicate bedrock specific capacity of 0.009–0.012 L/s·m, HCO<sub>3</sub>-Ca water type with 0.703 g/L mineralization, confirming extremely weak water-bearing capacity. Field observations further validate low water-richness of overlying bedrock (see Fig. 2).

**Table 1.** Statistics on Water Level Changes in the Study Area (m)

Year	2008	2009	2010	2011	2012	2013	2014	2015	2016	2017	2018	2019	2020	2021	2022	2023	2024
Elevation	-83.8	-85.9	-87.0	-87.9	-88.5	-89.8	-90.3	-90.3	-90.2	-91.0	-92.0	-93.4	-93.7	-93.9	-94.1	-94.3	-94.3

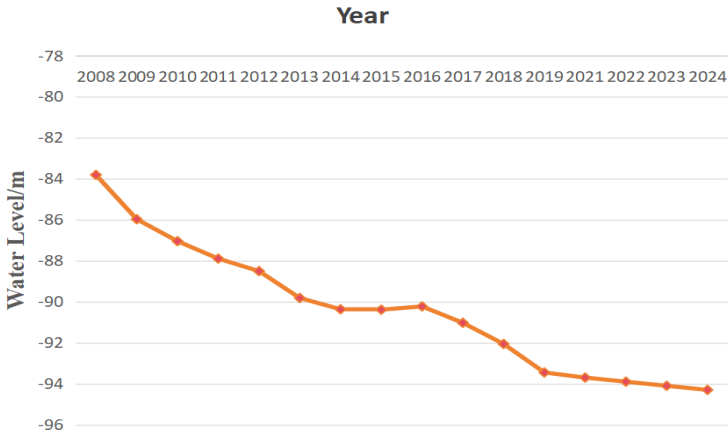


Fig. 2. Hydrological Change Trends in the Area

### 3 Theoretical Analytical Calculation

Based on Protodyakonov’s arch theory, the roof of an unsupported or long-term unmaintained roadway will form a natural collapse arch, which can be categorized into natural arch, pressure arch, and failure arch [1]. The studied scenario aligns with the mechanical characteristics of the pressure arch, calculated as follows:

Pressure Arch Model: When lateral pressure acts on rock strata, even reinforced roadways experience sliding of sidewalls along surfaces inclined at an angle approximately equal to the internal friction angle ( $\varphi$ ), forming a pressure arch. The arch height ( $h$ ) is given by the classical Protodyakonov formula. Please refer to “Equation (1)”:

$$h_1 = \frac{b_1}{f} = \frac{b + a \cdot \tan\left(45^\circ - \frac{\varphi}{2}\right)}{f} \tag{1}$$

Calculated based on the largest roadway section size of 3.6 m×2.5 m,  $b = 1.8\text{m}$ ,  $a = 2.5\text{m}$ ,  $\varphi = 37^\circ$ ,  $f = 1$ . Thus, the failure height of the roadway roof can be calculated as 3.1 m. When excavating through a fault, the failure height of the surrounding rock is 1.5 times that under fault-free conditions [2-3]. Assuming the maximum designed width and height, the predicted failure height of the roadway roof is 3.1 m, so the failure height of the surrounding rock during fault-crossing roadway excavation is 4.65 m. For safety, a safety factor of 2 is applied, and the maximum failure height is taken as 9.3 m.

## 4 Numerical Simulation

The numerical model in this study is developed using UDEC 6.0 software (Itasca Corporation). It effectively simulates the mechanical behavior of discontinuous media under both static and dynamic loading conditions. UDEC incorporates 7 types of geotechnical material models and 5 types of joint models, enabling it to replicate the mechanical behavior of rock strata under diverse geological conditions. Additionally, the software supports quantitative analysis and real-time monitoring of stress, strain, and displacement at any point within the model. Data visualization is achieved through intuitive graphical representations, ensuring clear and accessible presentation of results .

### 4.1 Establishment of the Numerical Model

According to the depositional characteristics of the overlying strata above the working face, the coal seam and the roof/floor rock strata in the working face are treated as horizontal strata (with a dip angle of  $0^\circ$ ) to facilitate model construction. Based on the actual engineering geological and technical conditions of roadway excavation in the working face, a numerical model with a bedrock thickness of 25 m was established. The thickness of Coal Seam 3 is 8.5 m, and the thickness of the floor rock strata above Coal Seam 3 in the model is uniformly 40 m. The model adopts a plane strain model, with dimensions (length  $\times$  height) of 400 m  $\times$  100.5 m for the 25 m-thick bedrock model. Zero-displacement boundary conditions are applied to the bottom boundary, left boundary, and right boundary of the model, specifically: The bottom boundary is fully constrained ( $u=0$  and  $v=0$ ); The left and right boundaries are single-constrained ( $u=0$ ,  $v \neq 0$ ); The top boundary is a free boundary with no constraints. The rock strata above the top boundary are applied as external loads on the model's top boundary.

### 4.2 Simulation Process of Working Face Roadway Excavation

Based on the actual engineering geological and technical conditions of roadway excavation in the 7-1 working face, numerical simulation software was used to reproduce the excavation process of the crossheading in the 7-1 working face. The simulation was conducted in four steps: first, simulating the mining process of the East 5-1 working face; second, simulating the mining process of the East 5-4 working face; third, simulating the mining process of the 8-1 working face; and fourth, simulating the excavation process of the roadway in the 7-1 working face. After the final excavation, the model was run until equilibrium was achieved. The specific simulation results are shown in Figure 3.

As indicated in the figure, since both the transportation roadway and the track roadway of the 7-1 working face are located within the stress concentration zone of the coal pillar outside the goaf, plastic failure occurs in the regional coal pillar and rock strata within a certain range. By integrating the distribution of overlying strata caving and plastic failure, it is concluded that when excavating a roadway in the coal pillar of

the stress concentration zone close to the goaf, the maximum failure height of the overlying strata is approximately 3.0 m.

Additionally, based on conventional engineering experience and peer consultations, the failure range of surrounding rock under similar conditions generally does not exceed the roadway width of 3.6 m, consistent with the simulated outcome. Considering the above analyses, the larger value of 3.1 m is adopted for the surrounding rock failure height in normal roadway excavation, while it increases to 4.65 m when crossing faults<sup>[3-4]</sup>. With a safety factor of 2, the maximum failure height is determined to be 9.3 m for the 7-1 working face roadway excavation (see Fig. 3).

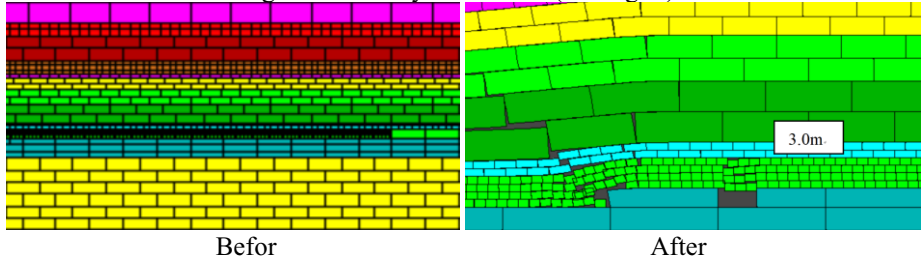


Fig. 3. Simulation Result Diagram

## 5 Safety Evaluation and Measures

### 5.1 Safety Evaluation of Roadway Excavation

(1) The overlying Quaternary in the study area serves as an aquiclude, blocking hydraulic connections between the lower Quaternary and other aquifers. Borehole pumping tests, in-mine exploration hole water inflow data, and water level observations confirm that the basal Quaternary aquifer has low water abundance, posing no water-inrush risk to the excavation face.

(2) A 1.5-m-thick clay layer at the base of the Quaternary effectively prevents downward seepage from the basal aquifer while restricting the failure height of the excavated roof strata, enhancing mining safety<sup>[4]</sup>.

(3) The working face bedrock exhibits a "soft-upper-hard-lower" structure, which inhibits fracture development and further improves excavation safety.

(4) The thinnest roof bedrock in the 7-1 working face is 22 m, leaving a 12.7-m thick protective bedrock above the roadway roof based on previous failure predictions, posing no direct water inflow threat.

### 5.2 Safety Technical Measures

Install reliable lighting, signaling, and communication systems in the development area to ensure seamless communication with the surface control center. If water inflow is detected during excavation, on-site personnel must immediately report to the mine dispatch and chief engineer and implement emergency protocols. Develop safety protocols integrating flood escape routes, accompanied by detailed evacuation plans.

Enhance monitoring of hydrological observation wells in the basal aquifer during excavation, reporting and addressing anomalies promptly.

## 6 Conclusions

- (1) The overlying Quaternary (156.2–180.0 m, avg. 164.6 m) has an upper aquiclude and a low-yield lower aquifer. A 1.5-m clay layer at the base blocks hydraulic connections with overlying strata and bedrock.
- (2) The thinnest bedrock (22.0 m) features 38.2% mudstone and a "soft-upper-hard-lower" structure, restricting overburden failure post-excavation.
- (3) Modeling shows failure heights of 3.1 m (normal) and 4.65 m (fault zones); with a safety factor of 2, the max height is 9.3 m, leaving 12.7 m of protective rock.
- (4) Site-specific safety measures are proposed for safe excavation.

## 7 Acknowledgement

**Funding Support:** This project is funded by the Zaozhuang Science and Technology Innovation Project (project number: 2024FG21); project title: "Research on the Development Path for Empowering Tengzhou's High-end Machine Tool Industry with New Productive Forces".

## References

1. Wenquan Z, Analytic Estimate of Floor Destroying Depth under Arch Structure of Overlying Rock of Coal Seam[C]. Progress in Safety Science and Technology (Vol.IV) Part A--Proceedings of the 2004 International Symposium on Safety Science and Technology, 2004:926-930.
2. Zhida L, Weikui L, Guibin Z. Numerical Simulation Study on the Influence of Faults on Water Inrush in the Roof of Working Faces[J]. Shandong Coal Science and Technology, 2021, 39(4): 165-167, 171.
3. Wei L, Guangpeng Z, Zhida L, et al. Numerical Simulation Study on the Reasonable Width of Fault Protection Coal Pillar and Working Face[J]. Mining Safety and Environmental Protection, 2014, 41(1): 16-19.
4. Peisen Z, Wenquan Z; Safety Analysis for Pillar of Ally Exploitation Laneway In Extreme Close Distance Coal Seam[C]. Progress in Safety Science and Technology (Vol.IV) Part A--Proceedings of the 2004 International Symposium on Safety Science and Technology, 2004:915-919.

**Open Access** This chapter is licensed under the terms of the Creative Commons Attribution-NonCommercial 4.0 International License (<http://creativecommons.org/licenses/by-nc/4.0/>), which permits any noncommercial use, sharing, adaptation, distribution and reproduction in any medium or format, as long as you give appropriate credit to the original author(s) and the source, provide a link to the Creative Commons license and indicate if changes were made.

The images or other third party material in this chapter are included in the chapter's Creative Commons license, unless indicated otherwise in a credit line to the material. If material is not included in the chapter's Creative Commons license and your intended use is not permitted by statutory regulation or exceeds the permitted use, you will need to obtain permission directly from the copyright holder.

